



AN ASSESSMENT OF LAND SURFACE TEMPERATURE DYNAMICS DUE TO URBANIZATION IN NATIONAL CAPITAL REGION OF INDIA

Kumar Anandam*¹, Krishan Kumar¹, Deepak Singh¹, Amit Kumar² and Vinod Kumar Jain¹

¹School of Environmental Sciences, Jawaharlal Nehru University, New Delhi, India

²Material Science, Engineering, Radio and Atmospheric Science Division, National Physical Laboratory, New Delhi, India

ARTICLE INFO

Article History:

Received 15th September, 2017

Received in revised form 25th

October, 2017

Accepted 23rd November, 2017

Published online 28th December, 2017

Key words:

Landsat; Land surface temperature; LULC; Maximum Likelihood Classifier; NCR

ABSTRACT

The current study analyses the satellite retrieved Land Surface Temperature (LST), LULC change in the National Capital Region (NCR) of India. A well-known parametric Maximum Likelihood Classifier algorithm (MLC) was employed for supervised spectral signature extraction of all Landsat images for five LULC classes such as Built-up area, Water body, Green vegetation, Rocky area and Bare land. After post-classification, results showed significant increase in area has been noticed from 2003 to 2009 with 75.68, and 26.72 % for Built-up area and Green vegetation, respectively while the Rocky area and Bare land decreased by 35.25% and 03.73%, respectively. In between 2009 to 2014 Built-up area and Green vegetation area cover further increases by 14.81 and 34.20% respectively while the Rocky area decreases by 50.17%. The mono-window algorithm has been used to retrieve LST map from the thermal band of Landsat level 1 data. The local pattern of LST was classified into four broad class (Lower, Moderate, High and Extreme) based on standard deviation. Results showed significant spatio-temporal change in LST in relation to different LULC types. Green vegetation, Built-up area and Rocky areas belong to Lower, Moderate and High LST class respectively. Similarly increasing trend has been observed for Built-up area and Green vegetation with area covered under Lower and Moderate class during studied period in NCR.

Copyright©2017 **Kumar Anandam et al.** This is an open access article distributed under the Creative Commons Attribution License, which permits unrestricted use, distribution, and reproduction in any medium, provided the original work is properly cited.

INTRODUCTION

In the recent decades, industrial and service based economic developments along with corresponding increase of population have rapidly changed the Land-use and Land-cover (LULC) composition in the urban area. Urbanization is one of the most important processes for the human needs which lead to losses of vegetation cover, agricultural area and habitat destruction (Balcik, 2013; Dewan and Yamaguchi, 2009; Ward *et al.*, 2016). More than half (54%) of global population live in urban area or cities, which cover less than 3% of total earth's land surface area (Liu *et al.*, 2014; United Nation 2014). The increasing pace of global urbanization influences the net productivity, biodiversity, weather and climate at local, regional and global arena (Han and Xu, 2013; Lasanta *et al.*, 2012; Mohan and Kandya, 2015; Vorovencii 2015; Yin *et al.*, 2010). The conversion of one type of LULC to another affects the process of energy exchange between the terrestrial land and the atmosphere (Wang *et al.*, 2016). Expansion of urban areas in developing countries in recent decades prompted the scientific community to identify and quantify the changes in

LULC composition has changed during rapid expansion of urban area at the cost of natural LULC and influenced the local meteorological and climatological parameter such as Land Surface Temperature (LST) and air temperature (Ding *et al.*, 2013; Feizhang *et al.*, 2016; Jones *et al.*, 1990; Wang *et al.*, 2016; Weber *et al.*, 2014; Zhang *et al.*, 2013). LST is considered as one of the key tools in order to study climatic variability and other environmental parameters (Ayanlade, 2016; Feng *et al.*, 2014; Nguyen *et al.*, 2015; Pichierri *et al.*, 2014). The changes in LULC influence the LST due to the partitioning of sensible and latent heat flux of different LULCs (Dubreuil *et al.*, 2011).

The enhancement in scientific development of remote sensing techniques by different national and international agencies provides an approach for precise spatio-temporal assessment of land surface phenomenon. Many researchers have employed remotely sensed images such as Landsat TM/ETM⁺ (Thematic Mapper and Enhanced Thematic Mapper), MODIS (Moderate Resolution Imaging Spectro-radiometer) spatial resolution 1 km and ASTER (Advanced Spaceborne Thermal Emission and Reflection) spatial resolution 90 m to retrieve LST (Brabynet *et al.*, 2013; Ding *et al.*, 2013; Jimenez-Munoz *et al.*, 2003; Kloog *et al.*, 2012; Liu *et al.*, 2006; Sobrino *et al.*, 2004;

*Corresponding author: **Kumar Anandam**

School of Environmental Sciences, Jawaharlal Nehru University, New Delhi, India

Tomlinson *et al.*, 2012). Many studies reported that TM/ETM⁺ data set is one of the best data available to study the association between LULC composition and LST because it has fine spatial resolution and delivers multiple spectral range band data simultaneously (Ding *et al.*, 2013;Feng *et al.*, 2014;Sobrino *et al.*, 2004).

Landsat project is a joint initiative between USGS and NASA, which provides calibrated high spatial resolution data of world for 42 years to the scientific community, national security agencies and academia. LULC composition changes and its corresponding LST is derived from Landsat level 1 image dataset which is processed according to information provided in metadata file and Landsat data user Handbook. Geographical information system (GIS) like ArcGIS {Environmental Systems Research Institute (ESRI), 380 New York Street, Redlands, CA} and Environment for Visualizing Image Software {(ENVI) Exelis Visual Information solution Inc, Boulder CO, USA} are efficient tools to visualize, analyze and for data interpretation to establish relationship, pattern and trend of satellite dataset (Dewan and Yamaguchi, 2009).

Most of the previous studies revealed that spatial and temporal change of LULC had a predominant effect on LST because each and every land cover type has distinct emissivity (Carlson *et al.*, 1997;Ding *et al.*, 2013;Mallick *et al.*, 2008;Rozenstein *et al.*, 2015). Numbers of studies have been carried out in order to evaluate the variability and relationship of LULC change with LST in past decade (Han and Xu, 2013;Jimenez-Munoz *et al.*, 2003; Liu *et al.*, 2006; Wang *et al.*, 2016). The recent urbanization and industrialization phenomenon have encouraged scientists, academicians, policy makers and city planners to assess the magnitude of LST change with different LULC types.

The present study tries to find out the LULC composition changes and its influence on spatio-temporal LST which occurred during 2003 to 2014 in National Capital Region (NCR) of India. Three prominent objectives of the present study are: firstly, quantification of spatio-temporal changes of five classified major LULC types occurred during 2003 to 2014 from multispectral band data of Landsat images. Secondly, spatio-temporal changes of LST over stipulated time period which is retrieved from Thermal infra-red band has been also analyzed. Thirdly, relationship has been investigated between spatio-temporal LULC composition changes due to urbanization with LST class.

METHODOLOGY

Study area

The study area, National Capital Region (NCR) of India is located between latitude 28° 10' 00" N to 29° 00' 00" N and longitude between 76° 50' 00" E to 77° 35' 34" E (Fig. 1) and altitude lies between 213 and 305 m above msl. NCR is surrounded by Indo-Gangetic alluvial plain in east and north, Thar Desert in west and by Aravalli Hill range in south. It lies in composite climatic zone with annual rainfall of 714 mm, mostly 3/4th rainfall occurs in July to September months. During the summer months, temperature ranges between 40-45 °C whereas winter temperature falling to 4-5 °C in months of December-January. In recent years, NCR is one of the fastest expanding cities in India in terms of population growth. According to Census conducted in 2011, decadal population growth rate is 20.96 % in between 2001 to 2011. The rapid

population growth has accelerated urbanization which resulted in intensive changes of LULC types which has led to change in local meteorological parameter such as LST.

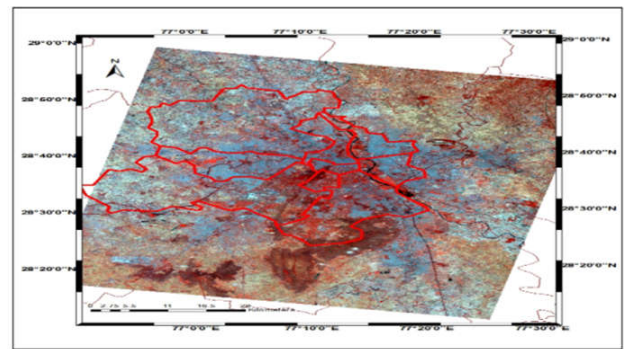


Fig 1 Map showing the NCR of India (FCC image of Landsat 8) in May 2014

Data Source

Three different Landsat L₁T data [(Path146/Row040) (Landsat 7 ETM⁺ (10 May 2003), 5 TM (18 May 2009) and 8 OLI (16 May 2014)] have been taken from USGS online archived GLOVIS (<http://glovis.usgs.gov/>) for NCR of India. Landsat 5 TM data consist of six bands in the Visible Region (VR) and Near Infrared Region (NIR) with 30 m spatial resolution and one Thermal Infrared Region (TIR) with 120 m (resembled 30 m) spatial resolution. Landsat 7 provides eight bands, i.e. six each in the VR and NIR with 30 m spatial resolution, one TIR with 60 m (resampled 30 m) spatial resolution and one panchromatic band with 15 m spatial resolution (http://LANDSAT.usgs.gov/band_designations_LANDSAT_satellites.php). The OLI sensor gathers image of eight VR, NIR and short wave infra-red (SWIR) with a 30 m spatial resolution, one 15 m panchromatic and two 100 m (30m resampled) TIR bands (Landsat 8 data users' handbook). Landsat images are one of the most suitable data for LST analysis with LULC composition changes over time because fine spatial resolution in VR, NIR, SWIR and TIR spectral bands. The toposheets of Delhi-NCR region having 1:50000 scales have taken from Survey of India (SOI) outlet for year 2005.

Preprocessing of Image data

We have selected those image data which were acquired during no cloud cover (0-2 %), so minimize the atmospheric anomaly due to cloud. Landsat images are processed as absolute radiance using 32-bit unit floating point then convert to 16-bit integer (Digital Number unit) value in level 1 product (Landsat 7 and 8 Handbook). The conversion of integer value to original 32-bit unit floating point spectral radiance has been done by scaling factor allocated in metadata file of each band data in ENVI (Band Math tool) software using following equations.

Spectral radiance (L_λ) has been calculated using Digital Number (DN) of each band for ETM⁺ and TM Image Band by

$$L_\lambda = \frac{LMAX_\lambda - LMIN_\lambda}{QCALMAX - QCALMIN} \cdot (QCAL - QCALMIN) + LMIN_\lambda \quad (1)$$

where L_λ is Spectral radiance at the sensor's aperture in W/m².sr.µm, QCAL is the quantized calibrated pixel value in DN, LMIN_λ and LMAX_λ are the Spectral radiance that is scaled

to QCALMIN and QCALMAX respectively, in $W/m^2 \cdot sr \cdot \mu m$. QCALMIN means the minimum quantized calibrated pixel value corresponding to $L_{MIN\lambda}$ in DN which is 1 for LPGS (Level 1 Product Generation System) and NLAPS (National Landsat Archive Production System) products processed after 4/4/2004 is zero for NLAPS products processed before 4/4/2004, QCALMAX (the maximum quantized calibrated pixel value corresponding to $L_{MAX\lambda}$) in DN is 255.

These spectral radiance (L_λ) is converted to spectral reflectance (P_p) at top of the atmosphere (TOA) by using the eq:

$$P_p = \frac{\pi \cdot L_\lambda \cdot d^2}{ESUN_\lambda \cdot \cos \Theta_s} \quad (2)$$

Here, P_p (TOA Planetary Spectral Reflectance), d^2 is distance between Earth and Sun in astronomical units, $ESUN_\lambda$ (Mean Solar Exo-atmospheric irradiances) and Θ_s is solar zenith angle in degrees (Landsat 7 Handbook, Chander *et al.*, 2003).

For Operational Land Imager (OLI) 16-bit spectral radiance unit is directly converted to TOA reflectance by

$$P_p = \frac{M_p \cdot Q_{cal} + A_p}{\sin(\Theta)} \quad (3)$$

M_p is reflectance multiplicative scaling factor for the band; A_p is reflectance additive scaling factor for the band and Θ is solar elevation angle (Landsat 8 Handbook).

Image classification and accuracy assessment

A well-known parametric Maximum Likelihood Classifier algorithms (MLC) was employed for supervised spectral signature extraction of all images. In each composite bands, image 100 ROI (Region of Interest) were chosen for each LULC type having all spectral signature adequately represented in the training statistics. Different band combination (R.G.B) was employed for distinct LULC for ROI selection in Arc-GIS image classification tool (training sample manager) detail given in Table 1.

Table 1 RGB bands combination for ROI selection.

Landform	R.G.B bands combination for TM & ETM+ Image	R.G.B bands combination for OLI Image
Built-up Area	7.5.3	7.6.4
Water Bodies	4.5.3	5.6.4
Green Vegetation	4.5.1	5.6.2
Rocky Area	5.4.3	6.5.4
Bare Land	4.5.3	5.6.4

Five significant distinct LULC types (Built-up area, Water body, Green vegetation, Rocky area and Bare land) were identified in all three images acquired at above prescribed date (Table 2).

Table 2 Landform types for classification

LULC	Abbreviations	Descriptions
Built-up Area	BA	Road, Building and Residential area
Water Bodies	WB	River, Ponds and Drainage system
Green Vegetation	GV	Forest, Farmland tree, Roadside tree and Vegetation around water bodies.
Rocky Area	RA	Rocky area and Sparse scrub vegetation
Bare Land	BL	Dry desert land, Open un-vegetated land, Bare soil and Sandy area

The Built-up area (urban areas) is composed of road, building and all types of impervious surfaces. Water body class

included River, Ponds and Drainage system in NCR. Forest, Farmland tree, Roadside tree and Vegetation around water bodies were lie under Green vegetation class of LULC. The Rocky area situated at south to central ridge covered by sparse scrub vegetation showed distinct spectral signature identified in individual LULC. The Bare land included dry land, semi-dry agricultural land and barren land in urban area in study area.

Assessment of classification accuracy is indispensable for accurate estimation of change detection in each classified images. Accuracy assessment procedure has been carried out with assigned ancillary data such as digitized toposheet of NCR for 2005 and field data collected for different LULC in 2014 as reference. Firstly, 200 random points were created from subset image of study area and then assigned each random point a value from digitized toposheet (for TM and ETM+) and field collected data for OLI image. Extracting the value of each LULC type and to this assigned a random value from classified image has been done. Accuracy assessment was done to create confusion matrix between assigned point and extracted value of each LULC type. It was observed that the overall accuracy with Kappa coefficient for corresponding three classified images ETM+, TM and OLI are 0.91, 0.83, and 0.95, respectively. The detection of LULC changes over the studied time period has been carried out using a post-classification differentiation method by randomly selecting 10000 points in classified image.

Retrieval of LST and local pattern

The thermal Infrared band (10.4-12.4 μm) for TM and ETM+ band no. 6 (low gain) data and band 10 were used for OLI data for retrieval of LST. The extraction of LST has been carried out by using mono-window algorithm (Qin *et al.*, 2001) and conversion pathway described in Handbook of Landsat 7 and 8. Eq. 1 has been used for derivation of spectral radiance for TM and ETM+ band whereas for OLI band DN value was converted to spectral radiance by using following Eq. 4.

$$L_\lambda = M_L \cdot Q_{cal} + A_L \quad (4)$$

where L_λ is Spectral radiance in $W/m^2 \cdot sr \cdot \mu m$, Q_{cal} is level 1 pixel value in DN, M_L and A_L are multiplicative and additive scaling factor for the band 10th of OLI.

Further, the Brightness Temperature (BT) has been retrieved at TOA in Kelvin from spectral radiance using Eq. 5 under assumption of unity emissivity.

$$BT = \frac{K_2}{\ln \left(\frac{K_1}{L_\lambda} + 1 \right)} \quad (5)$$

where K_1 and K_2 are thermal conversion constant consisting of metadata file whose values are 660.76 and 1260.56 for TM band, 666.09 and 1282.71 for ETM+ band, and 774.89 and 1321.08 for OLI band in $Wm^{-2} sr^{-1} \mu m^{-1}$, respectively. The above derived BT does not reflect the LST value because each LULC has distinct emissivity. Therefore, the BT of black body should be translated into emissivity corrected LST by the following equation (Ding *et al.*, 2013)

$$LST = \frac{(BT)}{1 + \frac{\lambda(BT)}{\rho} \cdot \ln \epsilon} \quad (6)$$

Where ϵ is the Land Surface Emissivity (LSE), λ ($11.5 \mu\text{m}$ for TM/ETM⁺ and $10.6 \mu\text{m}$ for OLI) is wavelength of emitted radiance, $\rho = \frac{hc}{\lambda kT} = (1.438 \times 10^{-2} \text{ mK})/kT$, k is Stefan-Boltzmann constant, h is Planck's constant and c is the velocity of light. LSE with corresponding LULC type were estimated through relationship between emissivity and Normalized Difference Vegetation Index (NDVI). Empirical approaches applied to established relationship between NDVI and LSE reported by Eq. 7 (Ding *et al.*, 2013).

$$\epsilon = 0.004P_V + 0.986 \tag{7}$$

where ϵ is surface emissivity and P_V is the vegetation proportion. P_V was computed from NDVI using following Eq.8 (Carlson *et al.*, 1997).

$$P_V = \left[\frac{(\text{NDVI}) - (\text{NDVI})_{\min}}{(\text{NDVI})_{\max} - (\text{NDVI})_{\min}} \right]^2 \tag{8}$$

where NDVI, NDVI_{\max} [(ETM⁺=0.54) (TM= 0.60) and (OLI= 0.52)] and NDVI_{\min} [(ETM⁺= -0.05) (TM= -0.15) and (OLI= -0.12)] computed from spectral reflectance of band 4 (NIR) and 3 (red) in ETM⁺ and TM image. In OLI image, band 5 (NIR) and 4 (red) reflectance have been used for NDVI calculation in ArcGIS software.

$$\text{NDVI} = \frac{\Gamma(\text{NIR}) - \Gamma(\text{R})}{\Gamma(\text{NIR}) + \Gamma(\text{R})} \tag{9}$$

Local pattern of LST is determined by using classification technique in Arc-GIS software from above derived LST into four classes (Lower, Moderate, High and Extreme) based on one standard deviation from the mean shown in Table 3. The spatial distribution of LST closely associated with LULC stabilized through overlay (intersect tool) technique in Arc-GIS software by randomly selected 10000 points in each images (LULC type and LST images).

RESULTS AND DISCUSSION

Spatial and temporal change of different LULC

For the present study, May month has been selected because in this month, generally cleaner (cloud free) atmosphere and high air temperature exists which is suitable for studies related to surface phenomenon via satellite observation. Spatial pattern of distinct LULC type in between three different dates is shown in Fig. 2 & 3 within NCR. On the analysis, it was found that during the period 2003 and 2009, the built-up area expands from 5.84% to 10.26% (almost double) this expansion has occurred in periphery of the city mainly in east, north-west, south-west and south-east direction.

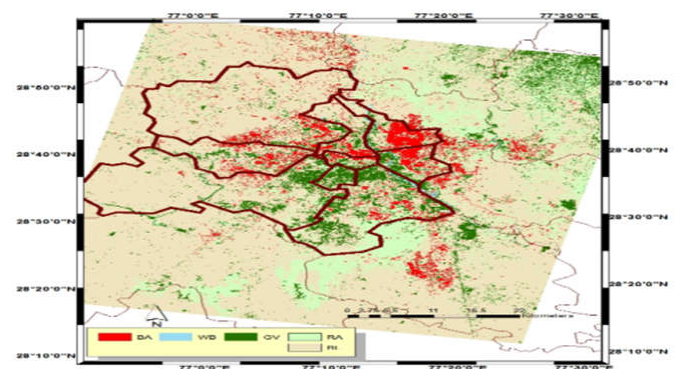


Fig. 2(a) Spatial pattern of LULC in May 2003

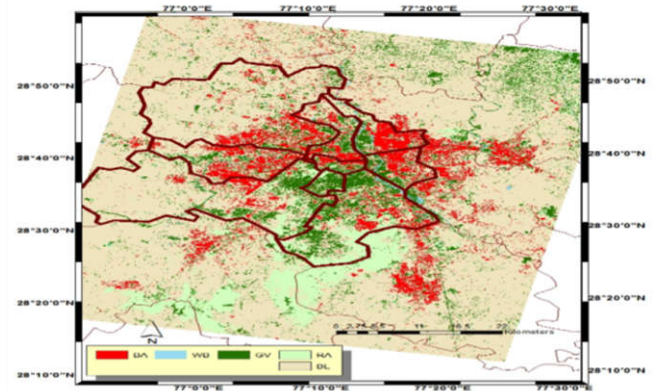


Fig. 2(b) Spatial pattern of LULC in May 2009.

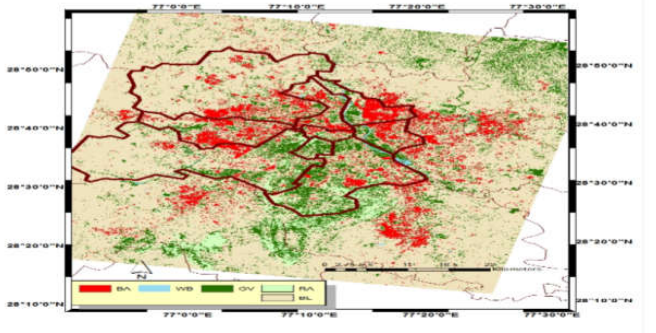


Fig. 2(c) Spatial pattern of LULC in May 2014.

The Green vegetation area has grown from 8.72 to 11.05 % primarily in central and south ridge area during the period 2003 to 2009. Rocky area has decreased from 12.99 to 8.41 % in between 2003 to 2009 period because of rapid expansion of urban Built-up area and conversion of sparse scrub vegetation into Green vegetation due to artificial plantation and natural process in studied area. Bare land and Water body contribution were 72.04 % and 0.39 %, respectively during 2003 which changed to 69.35 % and 0.91% during 2009, correspondingly. Bare land has been converted into Built-up area in periphery mainly in east and north-east direction which is mostly agricultural land and fallow land. In south, south-west and west direction Built-up area has developed at cost of Rocky area (ridge area) and dry non-arable land (desert land). Also there has been slight increase in Water body area due to increase in average rainfall from 6 mm in May 2003 to 65.8 mm rainfall occurred in 2009 (SA Delhi 2012). Due to this instantaneously rainfall most of the dry pits and dried ponds were full with water in 2009 which is detected as Water body area rather than Bare land detected in 2003.

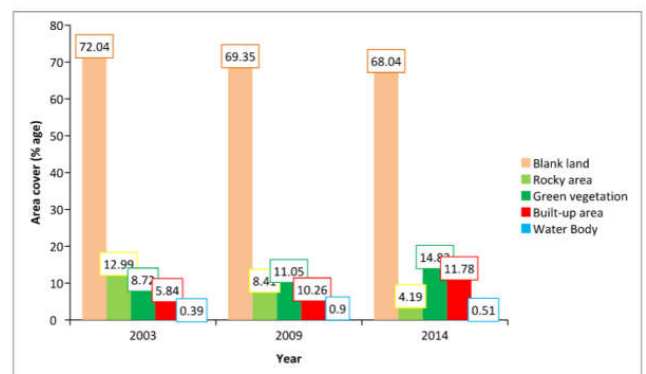


Fig. 3 Area covers under different LULC type in percentage during 2003-2014

In 2014, Built-up area, Water body, Green vegetation, Rocky area and Bare land contribution were observed to be 10.78, 0.51, 13.83, 3.19 and 71.67 %, respectively. It was found that Built-up area expansion rate in period between 2009 and 2014 reduced in comparison to 2003-2009 period. This was due to slow and stagnant economic growth and strict enforcement of government rules and regulations related to construction activities in these ecological sensitive zones such as ridge area in the foothills of Aravalli hill (SA Delhi 2012, 2014). Green vegetation zone has expanded in Rocky area due to conversion of scrub vegetation into Green vegetation in central and southern ridge area of NCR. Composition of LULC in north-eastern part has been gradually changed from sparse scrub vegetation in 2003 to Built-up area, Bare land and green agricultural land area during 2009. Overall, significant increase has been noticed from 2003 to 2014 with 101.00, 70.00 and 30.00% for Built-up area, Green vegetation and Water body, respectively. The Rocky area and Bare land decreased by 67.00% and 4.00%, respectively. These LULC change has highly influenced by population density change in NCR during 2000-2015. Spatial and temporal changes in satellite derived population density has followed similar pattern to spatio-temporal pattern of Built-up area during 2003-2014 (Kumar 2017). Summary of the composition of major LULCs change occurred over past 11 years is depicted in Fig. 4.

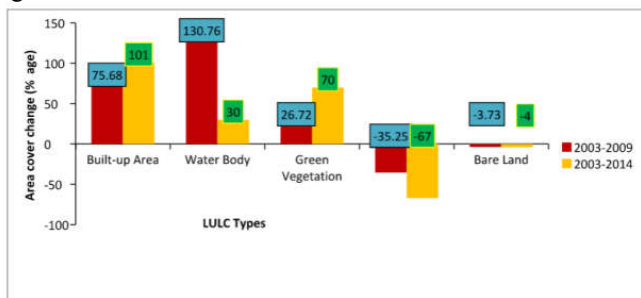


Fig. 4 Area cover change in different LULC in % age in during 2003-2009 and 2003-2014.

Spatial and temporal pattern of LST

The Spatial and temporal pattern of LST over Delhi-NCR for the months of May 2003, 2009 and 2014 respectively are shown in Fig.5 (a-c). It is observed that during May 2003, the LST ranged from 26.36 to 49.36°C with mean value of 39.65°C. While the corresponding LST ranges were observed to be 18.22 to 40.93°C (mean 31.44°C) and 24.30 to 44.58°C (mean 33.66°C) in the months of May 2009 and 2014 respectively. From the statistical parameters, it is observed that the month of May, 2009 is found to be cooler with minimum temperature of 18.22°C as compared to those for the months of May, 2003 for which the minimum temperatures were found to be 26.36°C. It is mainly due to the change in LULC pattern (Green vegetation area cover increase during 2003-2009) over the Delhi-NCR. The calculation of LST statistics for Delhi-NCR for the months of May 2003, 2009 and 2014 are shown below (Table 3).

Table 3 Statistics of LST classification during 2003-2014

Classification statistics	10 May 2003	18 May 2009	16 May 2014
Max Temp (°C)	49.36	40.93	44.58
Min Temp (°C)	26.36	18.22	24.30
Mean±SD	39.65±3.79	31.44±3.18	33.66±1.87

Spatial pattern of LST was determined by classifying above derived LST in four classes on the basis of standard deviation (Low, Moderate, High and Extreme) as shown below (Table 4). The results of LST have been classified by adding and subtracting the standard deviation from the mean LST value using GIS software.

Table 5 Mean LST of different LULC types in May month in year 2003, 2009 and 2014

LULC	10 May 2003 (°C)	18 May 2009 (°C)	16 May 2014 (°C)
Built-up area	37.37	29.93	34.85
VWMA area	35.07	27.95	31.69
Rocky area with scrub vegetation	40.10	32.84	35.12
Dry Bare land	45.14	35.56	38.83

The LST classification (namely, Lower, Moderate, High and Extreme) of the study area are shown in Table 4. In the month of May 2003, it is observed that LST ranged in various classes i.e. Lower (26.00-36.00°C), Moderate (36.00-40.00°C), High (40.00-45.00°C) and Extreme (>> 45.00°C). Further, in the month of May 2009, the corresponding values of LST ranged from 18.00-28.00°C for Lower, 28.00-32.00°C for Moderate, 32.00-37.00°C for High and for Extreme >> 37°C. In addition, in the month of May 2014, the LST values observed in different classes were found to be Lower (24.00-32.00°C), Moderate (32.00-35.00°C), High (35.00-38.00°C) and Extreme (>> 38°C) respectively.

The spatio-temporal maps of LST are shown in Fig 6 (a-c) which describes the distribution patterns of different LST classes over the national capital region of India. Distinct temperature ramp was observed among LULC types perceived on the LST maps. It can be seen from the LST maps that the moderate to high scale LST expanded from center to periphery during the years 2009 and 2014 as compared to that of year 2003 because of increased built-up area at that region. Extreme LST range was shrinking gradually in western and southern part of the study area in stipulated time period because of the conversion of sparse scrub vegetation land (rocky area and desert area) into either green vegetation covers or built-up area. Lower and Moderate LST range cover was expanded from the central part of Delhi and north-eastern region lying to Delhi’s surroundings (along the bank of Yamuna River) to the north region in the surroundings of Delhi from May 2003 to May 2009. While in the month of May 2014, Lower and Moderate LST range cover were found to be further expanded towards south-west region in Delhi’s surroundings.

Association of LST with LULC

In this section, association of LST with different LULC has been evaluated. Many studies have reported that LST is closely associated with different LULC types such as built-up area, vegetation area, moist soil (agricultural land) and dry land (desert and rocky area) (Jones *et al.*, 1990, Pichierriet *et al.*, 2012, Zhang *et al.*, 2013). Therefore, it is important to investigate the relationship between different LULC and LST distribution pattern in the rapidly expanding NCR region of India. The spatial distribution of LST closely associated with LULC in the present study. This association was established through overlay (intersect tool) technique in Arc-GIS software by randomly selected 10000 points in each images (LULC type and LST images). Average LST of different LULCs and

corresponding classes of LST are shown in Table 5 and Table 6 respectively.

Table 6 LST class with different LULC types in May month in year 2003, 2009 and 2014.

LST Class	10 May 2003	18 May 2009	16 May 2014
Lower	VWMA area	VWMA area	VWMA area
Moderate	Built-up area	Built-up area	Built-up area
High	Rocky area with scrub vegetation	Rocky area with scrub vegetation	Rocky area with scrub vegetation
Extreme	Dry Bare land	Dry Bare land	Dry Bare land

In the month of May 2003, the mean LST were found to be 37.37°C, 35.07°C, 40.10°C and 45.14°C for built-up area, Green vegetation area including water bodies and Moist Agricultural land (VWMA area), Rocky area and dry Bare land respectively, which suggested that Built-up area, VWMA area, Rocky area and dry Bare land comes under Moderate, Lower, High and Extreme LST Class range respectively.

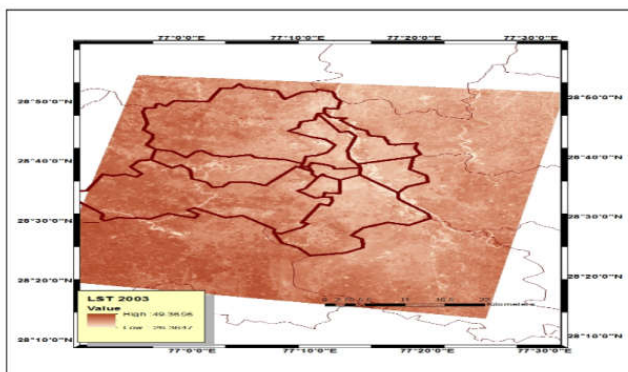


Fig. 5(a) LST during May 2003 in Delhi-NCR

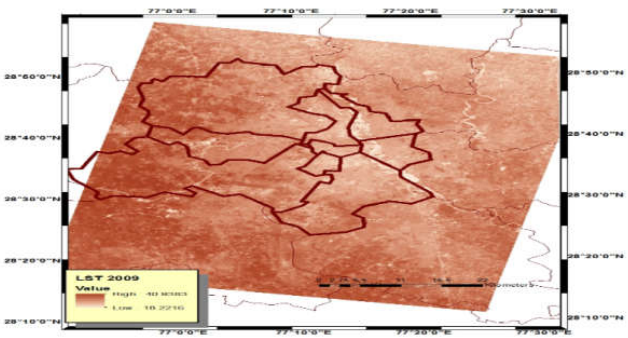


Fig. 5(b) LST during May 2009 in Delhi-NCR

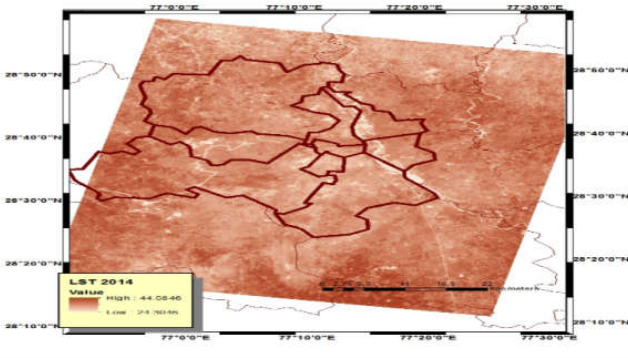


Fig. 5(c) LST during May 2014 in Delhi-NCR

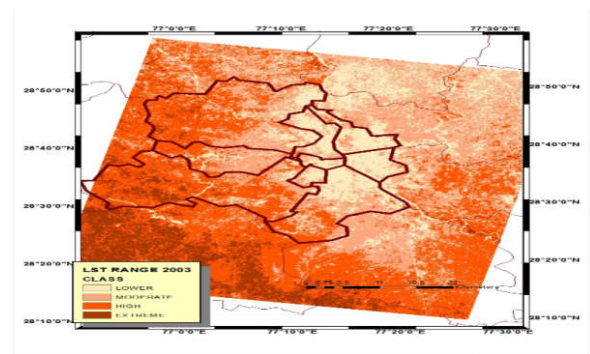


Fig 6 (a) Spatial pattern of LST class in 2003.

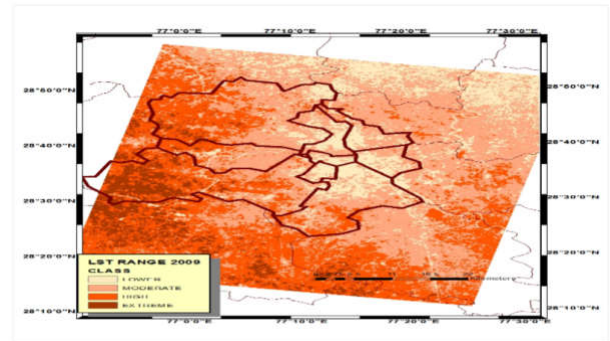


Fig. 6(b) Spatial pattern of LST class in 2009

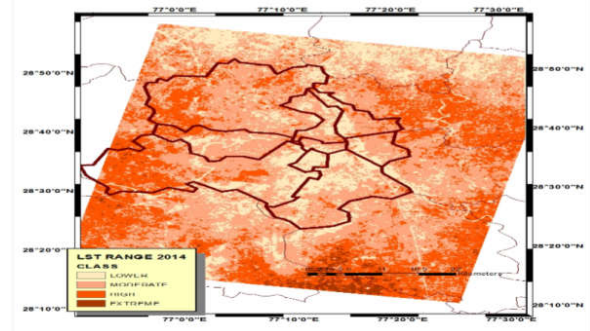


Fig 6(c) Spatial pattern of LST class in 2014.

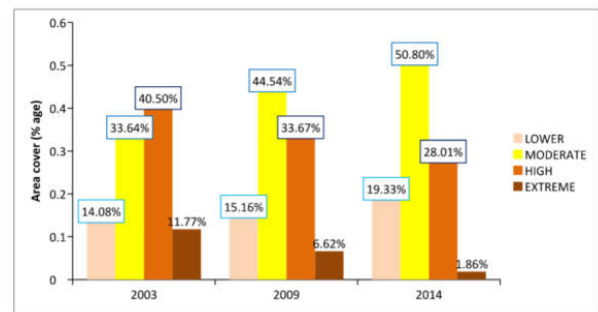


Fig. 7 LST area covers in percentage by different LST class during 2003-2014

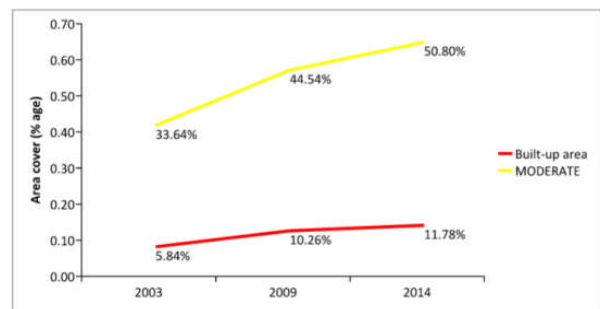


Fig. 8(a) A trend showing percentage of area cover by moderate LST class with built-up area cover during 2003-2014

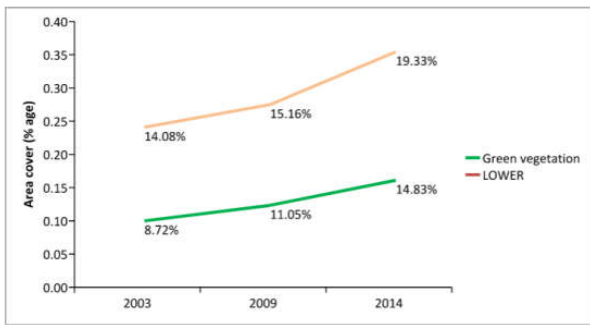


Fig. 8(b) A trend showing percentage of area cover by lower LST class with Green Vegetation cover during 2003-2014

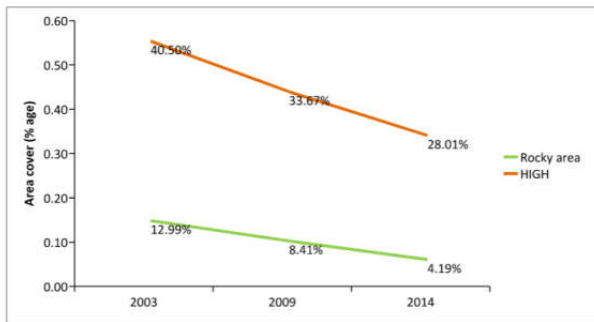


Fig. 8(c) A trend showing percentage of area cover by high LST class with Rocky area cover during 2003-2014

The results were found to be similar for the month of May 2009 as compared to those of May 2003. The Built-up area belong to moderate LST Class with mean temperature 29.93°C and other LULC types VWMA area belonged to lower (mean LST 27.95°C), rocky area belonged to high (average LST 32.84°C) and desert area belonged to high (average LST 35.56°C) LST Class respectively. Further, it can be observed during 2014, built-up area (mean LST 34.85°C) LST belonged to Moderate class, Rocky area belonged to high class (mean LST 35.12°C), VWMA area belonged to lower class (mean LST 31.69°C) and dry Bare land (mean LST 38.83°C) belonged to extreme LST Class respectively.

The percentage of area cover by different LST class is shown in Fig. 7. In 2003, the percentage of area cover for different LST class cover comprise Lower (14.08%), Moderate (33.64%), High (40.50%) and Extreme (11.77%) over the study area. In the year 2009, dynamic changes were observed in the area cover of different LST class i.e. Lower (15.16%), Moderate (44.54%), High (33.67%) and Extreme (6.62%) respectively. In the year 2014, total 70.83% area lied under two LST class i.e. Lower (19.33%) and Moderate, (50.80%), as compared to other two class i.e. High (28.01%) and Extreme (1.86%). It is observed that during the study period, area cover by Lower and Moderate class of LST is expanding while area cover by High to Extreme class decreases during this period (2003, 2009 and 2014).

From Fig. 2, it is clearly observed that the built-up area expanding the region lying north of Delhi and in eastern region of Delhi's surroundings which is dominated by agricultural land that leads to rise in average LST. Further, built-up expansion also occurred in south-west part of the city which was primarily covered by ridge and dry Bare land that leads to decrease in average LST over this region. Overall the mean LST for the entire NCR follow decreasing LST trend because of increased level of green vegetation cover during the months of May 2003, 2009 and 2014.

Overlaying (intersection) technique has been adopted to estimate the pattern of LST with LULC type's i.e. Built-up area, Green vegetation and Rocky area changes using ArcGIS software over the study area. From Fig.8 (a, b and c), it is clearly observed that the Moderate LST class pattern during 2003, 2009 and 2014 is closely associated with Built-up area pattern. The area by Moderate LST class was changed from 33.64% to 50.80%, which is followed by similar trend as of urban Built-up area that changed from 5.84% to 11.78% in between 2003 to 2014. It can be observed that urban area expansion highly influences the local LST dynamics.

Green vegetation area cover expands from 8.72% to 14.83% followed by similar increasing trends with Lower LST class from 14.08% to 19.33% between the years 2003 to 2014. The area cover by High LST class shrinks from 40.50% to 28.01% followed by similar decreasing trend to that of Rocky area which decreased from 12.99% to 4.19% in Delhi-NCR during 2003-2014.

Our study designated to the spatial and temporal role of LULC change on LST dynamics for rapidly expanding urban area (NCR) located in Indo-Gangetic region of India. Our study quantify of LST differences among different LULC types corroborate finding with other study carried out in different region of the world. Many studies showed in past that developed urban area (Built-up area) have higher temperature than adjacent open and green vegetation space area (Weng *et al.*, 2004;Bowler *et al.*, 2010;Lin and Lin, 2010;Cavan *et al.*, 2014). Our results showed that green area is increases during study period decipher increases the area of lower LST class provide an indicator by green infrastructure delivered a sustainable climate and economic realities and improving human well-being (Cilliers *et al.*, 2012; Schaffler and Swilling,2013).

CONCLUSIONS

LULC composition change in recent decade due to fast expansion of Built-up area in peripheral part of NCR had influenced the spatio-temporal pattern of local meteorological component. To stabilize a relation between different LULC compositions with spatio-temporal pattern of LST Landsat satellite images were used. LULC maps havederived through supervised classification (MLC) technique from multi spectral bands of Landsat image data. However, LST maps were derived from mono-window algorithm from thermal band of Landsat data.

From the present study, many conclusions are derived; Firstly, notable changes occurred in spatial pattern of LULC composition in the studied area during period between 2003 to 2009, 2003 to 2014 and 2009 to 2014. It is found that there is coherent increase in Built-up area and Green vegetation area due to conversion of ridge area (rocky area) and Bare landarea. Secondly, prominent change occurred in pattern of different class of LST in the studied time period. Spatio-temporal distribution of Extreme to high class of LST was dominant during 2003 in south-western and southern part of the NCR whereas moderate to high LST class in eastern and southern part during 2014. Area covered by Lower and Moderate class LST has increased by 37.28 and 25.43% respectively, whereas High and Extreme LST class cover area has decreased by 30.83 and 84.17% during 2003-2014 in NCR. Finally, LULC composition changes are predominant factor in LST anomaly

in stipulated time period has also been observed. Built-up area has expanded more in northern and eastern part of the city which leads to shifting of LST from lower to higher class. Urban Built-up area expansion follows similar increasing trend as Moderate LST class during study period. Lower LST class corresponding to Green vegetation concentrated in the central to northeast area of NCR during 2003 which gradually expanded to southern direction in later years due to conversion of scrub vegetation cover in ridge area into Green vegetation. The present study is the first comprehensive work which comprises both LST and LULC composition analysis in the NCR of India. It may provide better understanding of urbanization phenomenon with corresponding change in LULC composition and LST to policy makers and urban planners. For future studies, there is need for the availability of long term data with higher resolution for LULC composition and LST analysis for better understanding of urbanization process and its impact on environment.

Acknowledgements

The study is supported by a research grant (Senior Research Fellowship) from the University Grant Commission (UGC), New Delhi.

References

- Ayanlade A., 2016. Seasonality in the daytime and night-time intensity of land surface temperature in a tropical city area. *Science of the Total Environment*. 557-558, 415-424.
- Balçık, F. B., 2014. Determining the impact of urban components on land surface temperature of Istanbul by using remote sensing indices. *Environmental Monitoring and Assessment*. 186, 859-872.
- Bowler, D. E., Buyung-Ali, L., Knight, T. M., & Pullin, A. S. 2010. Urban greening to cool towns and cities: A systematic review of the empirical evidence. *Landscape and Urban Planning*. 97(3), 147-155.
- Brabyn, L., Zawar-Reza, Peyman., Stichbury, G., Cary, C., Storey, B., Laughlin, D. C. & Marwan, K. 2014. Accuracy assessment of land surface temperature retrievals from Landsat 7 ETM+ in the Dry Valleys of Antarctica using iButton temperature loggers and weather station data. *Environmental Monitoring and Assessment*. 186, 2619-2628.
- Cavan, G., Lindley, S., Jalayer, F., Yeshitela, K., Pauleit, S., Renner, F., et al., 2014. Urban morphological determinants of temperature regulating ecosystem services in two African cities. *Ecological Indicators*. 42, 43-57.
- Carlson, T. N., & Rizley, D. A. 1997. On the Relation between NDVI, Fractional Vegetation Cover, and Leaf Area Index. *Remote Sensing of Environment*. 62, 241-252.
- Chander, G., & Markham, B. 2003. Revised Landsat-5 TM Radiometric Calibration Procedures and Postcalibration Dynamic Ranges, IEEE Trans. *Geosciences and Remote Sensing*. 41(11), 2674-2677.
- Cilliers, S., Cilliers, J., Lubbe, R., & Siebert, S. 2012. Ecosystem services of urban green spaces in African countries-Perspectives and challenges. *Urban Ecosystems*. 16, 681-702.
- Dewan, A. M., & Yamaguchi, Y. 2009. Land use and land cover change in Greater Dhaka, Bangladesh: Using remote sensing to promote sustainable urbanization. *Applied Geography*. 29(3), 390-401.
- Ding, H., & Shi, W. 2013. Land-use/land-cover change and its influence on surface temperature: a case study in Beijing City. *Intl J Remote Sensing*. 34(15), 5503-5517.
- Dubreuil, V., Debortoli, N., Funatsu, B., Nédélec, V., & Durieux, Laurent. 2012. Impact of land-cover change in the Southern Amazonia climate: a case study for the region of Alta Floresta, Mato Grosso, Brazil. *Environmental Monitoring and Assessment*. 184, 877-891.
- Feng, H., Liu, H., & Wu, L. 2014. Monitoring the relationship between the land surface temperature and urban growth in Beijing, China. *IEEE J Applied Earth Observation and Remote Sensing*. 7, 4410-4019.
- Han, G., & Xu, J. (2013). Land surface phenology and land surface temperature changes along an urban-rural gradient in Yangtze River Delta, China. *Environmental Management*. 52, 234-249.
- Jime'nez-Munoz, J. C., & Sobrino, J. A. 2003. A generalized single-channel method for retrieving land surface temperature from remote sensing data. *Journal of Geophysical Research*, 108 (22), 4688.
- Jones, P. D., Groisman, P. Y., Coughlan, M., Plummer, N., Wang, W. C., & Karl, T. R. 1990. Assessment of urbanisation effects in time series of surface air temperature over land. *Nature*. 347, 169-172.
- Kloog, I., Chudnovsky, A., Koutrakis, P. & Schwartz, J. 2012. Temporal and spatial assessments of minimum air temperature using satellite surface temperature measurements in Massachusetts, USA. *Science of the Total Environment*. 432, 85-92.
- Kumar, A. 2017. An assessment of regional pattern of population induced land-use and landcover changes during last decade in ncr of India. *International Journal of Geology, Earth & Environmental Sciences*. 7 (2), 11-18.
- Landsat 7, Handbook, 1972. Science Data Users Handbook Landsat 7.
- Landsat 8, Handbook 2015. Science Data Users Handbook Ver 1.0 June, 2015.
- Lasanta, T., & Vicente-serrano, S. M. 2012. Remote Sensing of Environment Complex land cover change processes in semiarid Mediterranean regions: An approach using Landsat images in northeast Spain. *Remote Sensing of Environment*, 124, 1-14.
- Lin, B. S., & Lin, Y. J. 2010. Cooling effect of shade trees with different characteristics in a subtropical urban park. *Hort Science*, 45(1), 83-86.
- Liu, Y., Hiyama, T., & Yamaguchi, Y. 2006. Scaling of land surface temperature using satellite data: A case examination on ASTER and MODIS products over a heterogeneous terrain area. *Remote Sensing of Environment*. 127(105), 115-128.
- Liu, Z., He, C., Zhou, Y., & Wu, J. 2014. How much of the world's land has been urbanized, really? A hierarchical framework for avoiding confusion. *Landscape Ecology*. <http://doi.org/10.1007/s10980-014-0034-y>
- Mallick, J., & Kant, Y., & Bharath, B. D. 2008. Estimation of land surface temperature over Delhi using Landsat-7 ETM+. *J Ind Geophys Union*. 12(3), 131-140.
- Mohan, M., & Kandya, A. 2015. Impact of urbanization and land-use / land-cover change on diurnal temperature

- range : A case study of tropical urban airshed of India using remote sensing data. *Science of the Total Environment*. 506-507, 453-465.
- Nguyen, O.V., Kawamura, K., Trong, D. P., Gong, Z., & Suwandana, E.2015. Temporal change and its spatial variety on land surface temperature and land use changes in the Red River Delta, Vietnam, using MODIS time-series imagery. *Environmental Monitoring and Assessment*.187,464.
- Parenteau, M. P., & Sawada, M. C. 2012. The role of spatial representation in the development of a LUR model for Ottawa, Canada. *Air Quality, Atmosphere and Health*.5, 311–323.
- Pichierri, M., Bonafoni, S., & Biondi, R. 2012.Remote Sensing of Environment Satellite air temperature estimation for monitoring the canopy layer heat island of Milan. *Remote Sensing of Environment* 127,130-138.
- Qin, Z., & Karnieli, A. (2001). A mono-window algorithm for retrieving land surface temperature from Landsat TM data and its application to the Israel-Egypt border. *Int J Remote Sensing*, 22(18), 3719-3746.
- Rozenstein, O., Agam, N., Serio, C., Masiello, G., Venafra, S., Achal, S., & Karnieli, A. 2015. Diurnal emissivity dynamics in bare versus biocrusted sand dunes. *Science of the Total Environment*.506-507, 422-429.
- Sobrinoa, J. A., Munoz, J. C. J., & Paolini, L. 2004.Land surface temperature retrieval from LANDSAT TM 5. *Remote Sensing of Environment*. 90, 434-440.
- SA Delhi, Statistical Abstract of Delhi.2012. Directorate of Economics and Statistics, Govt. of NCT of Delhi.
- SA, Delhi, Statistical Abstract of Delhi.2014. Directorate of Economics and Statistics, Govt. of NCT of Delhi.
- Schaffler, A., & Swilling, M. 2013.Valuing green infrastructure in an urban environment under pressure: The Johannesburg case. *Ecological Economics*, 86, 246-257.
- Tomlinson, C. J., Chapman, L., Thornes, J. E., & Baker, C. J. 2012.Derivation of Birmingham’s summer surface urban heat island from MODIS satellite images. *International Journal of Climatology*. 32, 214-224.
- Vorovencii, I. 2015. Assessing and monitoring the risk of desertification in Dobrogea, Romania, using Landsat data and decision tree classifier. *Environmental Monitoring and Assessment*.187, 204.
- Wang, S., Ma, Q., Ding, H., & Liang, H. 2016.Detection of urban expansion and land surface temperature change using multi-temporal lands at images. *Resources Conservation and Recycling*, doi:10.1016/j.resconrec.2016.05.011.
- Ward, K., Lauf, S., Kleinschmit, B., & Endlicher, W. 2016. Heat waves and urban heat islands in Europe : A review of relevant drivers. *Science of the Total Environment*.569-570, 527-539.
- Weber, N., Haase, D., & Franck, U. 2014. Zooming into temperature conditions in the city of Leipzig : How do urban built and green structures in fluence earth surface temperatures in the city?, *Science of the Total Environment*. 496, 289-298.
- Weng, Q., Lu, D., & Schubring, J. (2004). Estimation of land surface temperature–vegetation abundance relationship for urban heat island studies. *Remote Sensing of Environment*, 89, 467-483.
- World Urbanization Prospects.2014.The Revision United Nations Department of Economic and Social Affairs/Population Division World Urbanization Prospects.pp xxi.
- Yin, J., Yin, Z., Haidong, Z., Xu, S., Hu, X., Wang, J., & Wu, J. 2011. Monitoring urban expansion and land use/land cover changes of Shanghai metropolitan area duringthe transitional economy (1979-2009) in China. *Environmental Monitoring and Assessment*.177, 609-621.
- Zhang, F., Tiyip, T., Kung, H., & Johnson, V. C. 2016. Dynamics of land surface temperature (LST) in response to land use and land cover (LULC) changes in the Weigan and Kuqariver. *Arabian Journal of Geosciences*.http://doi.org/10.1007/s12517-016-2521-8.
- Zhang, H., Qi, Z., Ye, X., Cai, Y., Ma, W., & Chen, M. 2013. Analysis of land use/land cover change, population shift, and their effects on spatiotemporal patterns of urban heat islands in metropolitan Shanghai, China. *Applied Geography*. 44, 121-133.

How to cite this article:

Kumar Anandam *et al* (2017) 'An Assessment of Land Surface Temperature Dynamics Due to Urbanization in National Capital Region of India', *International Journal of Current Advanced Research*, 06(12), pp. 8171-8179.
DOI: <http://dx.doi.org/10.24327/ijcar.2017.8179.1305>
